

RESEARCH

Open Access



LDLR c.415G > A causes familial hypercholesterolemia by weakening LDLR binding to LDL

Kaihan Wang^{1†}, Tingting Hu^{2†}, Mengmeng Tai^{1†}, Yan Shen¹, Haocheng Chai³, Shaoyi Lin^{1*} and Xiaomin Chen^{1*}

Abstract

Background Familial hypercholesterolemia (FH) is a prevalent hereditary disease that can cause aberrant cholesterol metabolism. In this study, we confirmed that c.415G > A in low-density lipoprotein receptor (*LDLR*), an FH-related gene, is a pathogenic variant in FH by in silico analysis and functional experiments.

Methods The proband and his family were evaluated using the diagnostic criteria of the Dutch Lipid Clinic Network. Whole-exome and Sanger sequencing were used to explore and validate FH-related variants. In silico analyses were used to evaluate the pathogenicity of the candidate variant and its impact on protein stability. Molecular and biochemical methods were performed to examine the effects of the *LDLR* c.415G > A variant in vitro.

Results Four of six participants had a diagnosis of FH. It was estimated that the *LDLR* c.415G > A variant in this family was likely pathogenic. Western blotting and qPCR suggested that *LDLR* c.415G > A does not affect protein expression. Functional studies showed that this variant may lead to dyslipidemia by impairing the binding and absorption of LDLR to low-density lipoprotein (LDL).

Conclusion *LDLR* c.415G > A is a pathogenic variant in FH; it causes a significant reduction in LDLR's capacity to bind LDL, resulting in impaired LDL uptake. These findings expand the spectrum of variants associated with FH.

Keywords Familial hypercholesterolemia, Low-density lipoprotein receptor, Pathogenic variant, Functional study

Introduction

Familial hypercholesterolemia (FH) is a hereditary metabolic disease typified by the dysregulation of cholesterol homeostasis [1]. Its principal features are highly elevated plasma low-density lipoprotein cholesterol (LDL-C), xanthoma of the skin and tendon, and the early onset of coronary heart disease [2]. Among patients with FH, a high level of plasma LDL-C is the main driver of cardiovascular risk [3]. In particular, those with homozygous FH may develop atherosclerosis as early as adolescence, affecting not just the arteries but also the valves, resulting in a heavy burden [4]. Clinically, FH is classified as either homozygous or heterozygous; the prevalence of heterozygous FH is about 1:313, while that of homozygous FH

[†]Kaihan Wang, Tingting Hu and Mengmeng Tai contributed equally to this work.

*Correspondence:

Shaoyi Lin
shaoyi_lin@hotmail.com
Xiaomin Chen
chxmin@hotmail.com

¹Department of Cardiology, The First Affiliated Hospital of Ningbo University, Ningbo, Zhejiang, China

²Department of Cardiology, The Quzhou Affiliated Hospital of Wenzhou Medical University, Quzhou People's Hospital, Quzhou, Zhejiang, China

³Department of Gastroenterology, Ningbo Ninth Hospital, Ningbo, Zhejiang, China



© The Author(s) 2024. **Open Access** This article is licensed under a Creative Commons Attribution 4.0 International License, which permits use, sharing, adaptation, distribution and reproduction in any medium or format, as long as you give appropriate credit to the original author(s) and the source, provide a link to the Creative Commons licence, and indicate if changes were made. The images or other third party material in this article are included in the article's Creative Commons licence, unless indicated otherwise in a credit line to the material. If material is not included in the article's Creative Commons licence and your intended use is not permitted by statutory regulation or exceeds the permitted use, you will need to obtain permission directly from the copyright holder. To view a copy of this licence, visit <http://creativecommons.org/licenses/by/4.0/>. The Creative Commons Public Domain Dedication waiver (<http://creativecommons.org/publicdomain/zero/1.0/>) applies to the data made available in this article, unless otherwise stated in a credit line to the data.

is 1:400,000 [5]. However, the early symptoms of FH are easily ignored, making the diagnosis of FH extremely difficult [6]. At present, the diagnosis rate of FH is very low in most countries and regions [7]. For example, it is <10% in the United States [8], 4% in Australia and New Zealand [9], 2% in South Africa [10], and even <1% in Russia, Latin America, and other countries [11]. Only a small percentage of those diagnosed with FH have undergone genetic testing. In most areas, the rate of genetic diagnosis is <5%, such as <5% in the United States [12] and <2% in Asia [13]. Based on the phenomenon of serious complications and the low diagnosis rate of FH, it is urgent to improve the diagnosis rate around the world. Because FH is a genetic disorder, cascade screening based on genetic diagnosis is the most effective way to improve the diagnosis rate [7].

The main pathogenic mechanism underlying FH is the incapacity of LDLR to remove LDL-C from the blood [14]. Under normal physiological conditions, the endoplasmic reticulum produces LDLR, which is then transported to the Golgi apparatus for glycosylation modification and carried to the plasma membrane. Finally, the LDLR on the plasma membrane binds to circulating LDL particles to promote endocytosis [14]. Once the vesicles encasing the LDLR-LDL complex have been absorbed into the cell, they merge with the endosome. In the acidic endosome, LDLR undergoes a conformational change and separates from the bound LDL [15]. This allows LDLR to return to the plasma membrane for later use or be directed to lysosomes for degradation by interaction with proprotein convertase subtilisin/kexin type 9 (PCSK9) [16]. In addition, LDLR on the cell membrane can also bind to circulating PCSK9 and be carried to lysosomes for degradation [17]. Circulating PCSK9 is secreted from hepatocytes and engages in several biological processes, such as lipid metabolism, immune response, hemostasis, glucose metabolism, and neuronal survival [18]. Among these, the regulation of plasma LDL-C concentrations is the most significant and extensively studied. The activity of PCSK9 is negatively correlated with LDLR density on the surface of hepatocytes and positively correlated with plasma LDL-C concentrations [19]. It has been shown that PCSK9 can form dimers and higher multimers through self-associating, which is influenced by concentration, temperature, and pH, and can increase LDLR degrading activity [20]. Besides, the half-life of circulating PCSK9 might be extended from 5 to 15 min by binding to LDLR [21]. Therefore, the increase in PCSK9 expression as well as the increase in activity and the decrease in degradation all lead to a decrease in LDLR, which increases the level of LDL-C in plasma. Any disruption in these processes leads to a notable and significant buildup of LDL-C in the plasma.

Similarly, genetic variants in FH patients cause anomalies in the receptor endocytosis pathway, which abnormally raises plasma levels of LDL-C [22], the extent of which differs between different countries and ethnic groups [23]. Of the previously mentioned genetic variants, variants in the *LDLR* gene account for the bulk of FH instances [24]. During the last few decades, plenty of studies on the *LDLR* variants of FH have been carried out globally, and many of them have been found in China. For example, in Han Chinese populations, there are 143 different variants of *LDLR* known to exist, and the four most frequent variants include c.986G>A, c.1747 C>T, c.1879G>A, and c.268G>A [25, 26]. In Hong Kong, there have been reports of 73 different *LDLR* variants, and the four most common variants included c.1241 T>G, c.1474 G>A, c.769 C>T, and c.1765 G>A [27]. Although more than 4,000 *LDLR* variants have been identified, less than 15% of them have been identified as benign or pathogenic through functional studies [28]. Theoretically, the clinical diagnosis cannot be verified until a genetic variant is identified and subsequently shown to modify the metabolism of LDL [29]. Therefore, it is vital to conduct genetic testing and functional studies on patients with FH, which can provide a strong basis for the diagnosis of FH.

In this study, genetic testing was conducted to identify variants associated with FH in a familial context. Subsequent *in silico* analysis and *in vitro* functional assessments were performed to identify the pathogenicity of *LDLR* c.415G>A. These findings contribute to broadening the spectrum of FH-related variants, thereby facilitating early diagnosis.

Methods

Study participants and blood sample collection

According to the diagnostic criteria of the Dutch Lipid Clinic Network (DLCN), individuals with scores of ≥ 8 points and their families were included in this study. After using DLCN diagnostic criteria to evaluate the participants, a family tree was built. Venous blood was collected from participants for a blood lipid analysis and subsequent whole-exome sequencing. Participants had completed informed consent forms, which were authorized by the First Affiliated Hospital Ethics Committee of Ningbo University.

Whole-exome sequencing

Venous blood samples were forwarded to the Beijing Genomics Institution (BGI, Wuhan, China) for whole-exome sequencing. After low-quality reads, adapters, and a high percentage of N-bases were removed from the raw sequencing data, alignments against the human reference genome hg19 sequence were generated using Burrows Wheeler Aligner [30]. Using the Genome Analysis

Toolkit (GATK), duplicate reads were tagged, and base mass value recalibration was performed. GATK4's HaplotypeCaller was used to find single nucleotide polymorphisms (SNPs) and InDels [31]. Rigorous filtering was applied to extract SNPs and InDels that are both highly dependable and of excellent quality.

Sanger sequencing

Utilizing the E. Z. N.P.® Blood DNA Mini Kit (D3392-02; Omega Bio-Tek, Norcross, GA, USA) for DNA extraction, which was then amplified using polymerase chain reaction (PCR). The total PCR system was 50 μ L, which includes 25 μ L of 2 \times ES Taq Master Mix, 2 μ L of forward primer (5'-CAGGACGAGTTTCGCTGCCAC-3'), 2 μ L of reverse primer (5'-ATCCGAGCCATCTTCGCAGT C-3'), 500 ng of DNA and enzyme-free water. After sending the PCR products to BGI for Sanger sequencing, data analysis was conducted using Chromas software.

In silico analysis

MutationTaster was used to predict the pathogenicity of point variants [32]. DynaMut was utilized to evaluate how point variants affected the stability and flexibility of proteins [33]. A normal mode analysis was used to determine the difference in free energy change ($\Delta\Delta G$) between the structures of the wild-type (WT) and the variant. ENCoM-based difference in vibrational entropy ($\Delta\Delta S_{Vib}$) was used to predict the difference in flexibility [34]. SnapGene v6.0.2 was employed to determine the conservation of protein sequences among species using the multiple sequence comparison by log-expectation (MUSCLE) algorithm.

Plasmid construction, cell culture, and transfection

Shanghai GeneChem Co. (Shanghai, China) completed the construction of human WT *LDLR* and *LDLR* c.415G>A with a FLAG epitope close to the N terminus in the GV208 vector. HEK293T cells were used for the plasmid transfection [35]. The cells were grown in Eagle media that had been modified by Dulbecco (high glucose) (Cytiva, Shanghai, China) containing 10% fetal bovine serum (Vivacell, Shanghai, China). For transfection, the cells were transfected with 2500 ng of plasmid DNA using Lipofectamine™ 3000 Reagent (Invitrogen, Shanghai, China) in a six-well plate.

Quantitative real-time PCR

Following transfection, TRIzol (Omega, Norwalk, CT, USA) was used to extract RNA, and the HiFiScript cDNA Synthesis Kit (CW2569M; CWBIO, Beijing, China) was used for reverse transcription. The Mastercycler® Nexus X2 (Eppendorf, Hamburg, Germany) was used to carry out quantitative real-time PCR (qPCR). TaqMan assays were employed for the detection of fluorescence. The

relative amplification efficiency of *LDLR* was established using the comparative Ct method. The primers used were as follows: *LDLR*, F-5'-AAGTGCATCTCTCGGCAGT T-3', *LDLR*, R-5'-CCACTCATCCGAGCCATCTT-3'; *GAPDH*, F-5'-GGAAATCGTGCGTGACATTA-3', R-5'-GGAAGGAAGGCTGGAAGAG-3'.

Western blotting

The cells were lysed using RIPA solution (Solarbio, Beijing, China), which contains inhibitors of phosphatase and protease. The proteins were boiled for 10 min with loading buffer (Solarbio, Beijing, China) in preparation for western blotting. Following 7.5% SDS/PAGE resolution, the samples were blotted onto PVDF membranes (Merck, Darmstadt, Germany). After using 5% skim milk to prevent non-specific binding, monoclonal mouse anti-FLAG (1:3000, F1804; Sigma, Shanghai, China) and monoclonal rabbit anti- β -actin (1:10000, AF7018; Affinity Biosciences, San Francisco, California, USA) primary antibodies were added, and the mixture was incubated for a whole night at 4 °C. Then, the samples were treated with the corresponding horseradish peroxidase-conjugated IgG for 60 min. Lastly, the immunoreactive proteins were identified using enhanced chemiluminescence.

Flow cytometry

Cells were added to a six-well plate with 0.05% trypsin and transferred into a 2 mL EP tube. Diluted rabbit anti-human *LDLR* monoclonal antibody conjugated with allophycocyanin (1:200, ab275614; Abcam, Cambridge, MA, USA) was added, and the mixture was maintained in the dark for an additional hour after blocking with 10% donkey serum for an hour at room temperature. The mean fluorescence levels from at least three replicate estimates were obtained using a Beckman CytoFlex S flow cytometer (Beckman Coulter, Shanghai, China). Data analysis was done with FlowJo software.

Immunofluorescence

After transfection, cells were fixed using 4% paraformaldehyde (P1110; Solarbio, Beijing, China). Following a wash with 1 \times PBS, the cells were blocked using a 10% goat serum solution to prevent non-specific binding. Next, mouse anti-flag antibody (1:3000, F1840; Sigma-Aldrich, Saint Louis, USA) was diluted in 1 \times PBS and incubated at 4 °C for 4 h, along with 20 μ g/mL labelled human plasma LDL (Dil-LDL; L3482; Thermo Fisher, Shanghai, China). After incubation, the cells were washed with 1 \times PBS and then treated with goat anti-mouse IgG conjugated with AlexaFluor488 (1:500, ab150113; Abcam, Cambridge, UK). After completing the staining of nucleus with 4',6-diamidino-2-phenylindole (DAPI), the cells can be observed under a LEICA TCS SP8 confocal laser scanning microscope.

In order to assess the uptake capacity of LDLR, transfected HEK293T cells were treated with 20 $\mu\text{g}/\text{mL}$ Dil-LDL for 4 h at 37 $^{\circ}\text{C}$. Similarly, confocal microscopy was used for analysis after washing with PBS, fixation with 4% paraformaldehyde, and DAPI labeling of cell nuclei.

Statistical analysis

All data was analyzed using GraphPad Prism (version 9.0.0; La Jolla, CA), and presented as means \pm SEM. Normal distribution was evaluated using the D'Agostino–Pearson omnibus normality test. Group differences were evaluated using a one-way ANOVA. $P < 0.05$ was used as the statistical significance criterion.

Results

Clinical data for the proband and his family members

The proband, a 39-year-old male who presented to the First Affiliated Hospital of Ningbo University due to chest tightness following physical activity. Coronary angiography revealed that his coronary artery was severely stenotic. Because of the early onset of atherosclerotic cardiovascular disease, FH was suspected; therefore, cascade screening was conducted. The biochemical results and DLCN scores for this family member are shown in Tables 1 and 2. Figure 1 depicts the pedigree. A positive family history of dyslipidemia was found in the pedigree analysis of the index case, which is compatible with an autosomal dominant mode of inheritance.

Genetic analysis and in silico screening

Owing to geographical constraints, blood samples were only obtained from three family members for whole-exome sequencing. The whole-exome sequencing data (Supplemental Table 1) were analyzed for variants in FH-related genes (*LDLR*, *APOB*, *PCSK9*, *LDLRAP1*). Two patients with FH in this family were identified to carry the missense variant *LDLR* c.415G>A (Fig. 2A). The presence of *LDLR* c.415G>A, which is found in exon 4 of the *LDLR* gene on chromosome 19 p13.2, was verified using Sanger sequencing (Fig. 2B). An interspecific sequence analysis revealed that the altered amino acid sequence is highly conserved (Fig. 2C). A MutationTaster analysis showed that the variant is pathogenic.

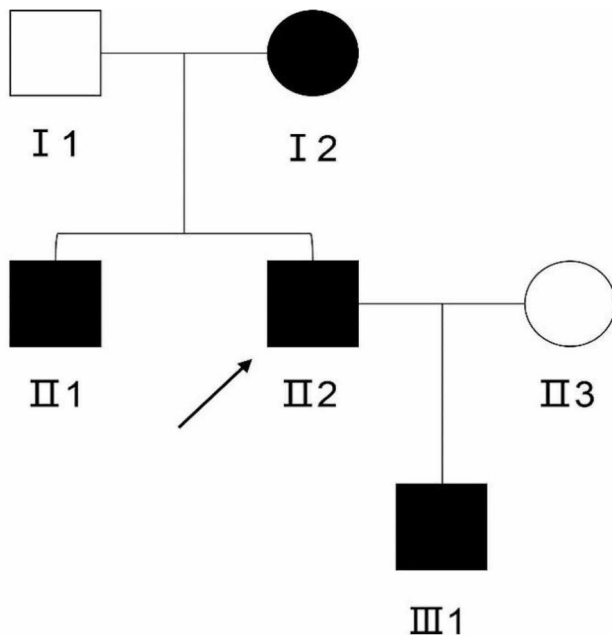
Additionally, the interatomic interactions of *LDLR* c.415G>A were assessed using DynaMut. The differences in interatomic interactions between the WT and variant are depicted in Fig. 2D. According to the predicted DynaMut $\Delta\Delta\text{G}$ values and $\Delta\Delta\text{S}$ ENCoM (Empirical Normal-Coordinate Analysis Method), the variant resulted in decreased molecular flexibility and increased stability of the LDLR protein.

Table 1 Clinical data of the proband and their first-degree relatives

Family member	age	gender	TG (mmol/L)	Reference range (mmol/L)	TC (mmol/L)	Reference range (mmol/L)	LDL-C (mmol/L)	Reference range (mmol/L)	HDL-C (mmol/L)	Reference range (mmol/L)	Coronary atherosclerosis	Xanthoma	history of atherosclerotic myocardial infarctions
I1	65	male	0.82	0.00–1.70	2.34	3.00–5.70	1.55	1.89–3.37	0.69	1.03–1.55	No	No	No
I2	65	female	0.74		8.84		7.96		1.02		No	No	Yes
II1	36	male	0.56		8.76		7.31		1.13		No	No	Yes
II2	39	male	0.87		6.51		4.45		1.15		No	No	Yes
III3	35	female	0.64		4.43		3.04		1.17		No	No	No
III1	7	male	0.52		6.18		5.01		1.05		No	No	No

Table 2 DLCN (Dutch Lipid Clinic Network) scores for the proband and his first-degree relatives

Diagnostic criteria of the Dutch Lipid Clinic Network	Score	Participant scores					
		I1	I2	II1	II2	II3	III1
Family History							
First-degree relative with known premature (< 55 years of age in men, < 60 years of age in women) coronary heart disease or first-degree relative with known low-density lipoprotein (LDL) cholesterol > 95th percentile by age and sex for country	1	0	1	1	2	2	1
First-degree relative with tendon xanthoma and/or arcus cornealis or children < 18 years of age with LDL cholesterol > 95th percentile by age and sex for country	2						
Clinical History							
Patient with premature coronary artery disease (age as above)	2	0	2	2	2	0	0
Patient with premature cerebral or peripheral vascular disease (age as above)	1						
Physical Examination							
Tendon Xanthomas	6	0	0	0	0	0	0
Arcus Cornealis at age ≤ 45 years	4						
LDL Cholesterol (mmol/L) (mg/dL)							
LDL-C ≥ 8.5 (330)	8	0	5	5	1	0	3
LDL-C 6.5–8.4 (250–329)	5						
LDL-C 5.0–6.4 (190–249)	3						
LDL-C 4.0–4.9 (155–189)	1						
DNA analysis							
DNA Analysis – functional mutation LDLR, APOB, and PCSK9	8	/	/	/	8	0	8
Total Score		0	8	8	13	2	12

**Fig. 1** Pedigree of the proband. The arrow indicates the proband. Dark circles or boxes in the lineage indicate subjects with FH. Circles represent females, and boxes represent males**LDLR c.415G > A variant does not change LDLR expression in vitro**

To confirm LDLR c.415G > A's effect on gene expression, HEK293T cells were transfected with plasmids carrying WT LDLR, variant LDLR, and blank. According to the immunofluorescence results, the transfection success rate was approximately 85% (Supplemental Fig. 1). qPCR

results, as illustrated in Fig. 3A, demonstrated that cells transfected with variant plasmids did not exhibit any differences in LDLR mRNA expression compared with those transfected with WT plasmids, whereas cells transfected with blank plasmids exhibited extremely low expression of LDLR mRNA. Western blotting results (Fig. 3B) revealed that LDLR protein expression was similar in the variant and WT groups but was essentially absent in the blank group. The flow cytometry results, as shown in Fig. 3C, demonstrated that the cell membrane in the blank group did not express the LDLR protein, while cell membranes in the variant and WT groups exhibited similar LDLR protein expression levels. The expression levels of the variant and WT groups did not differ statistically in any appreciable way. These findings show that gene expression is unaffected by the LDLR c.415G > A variant.

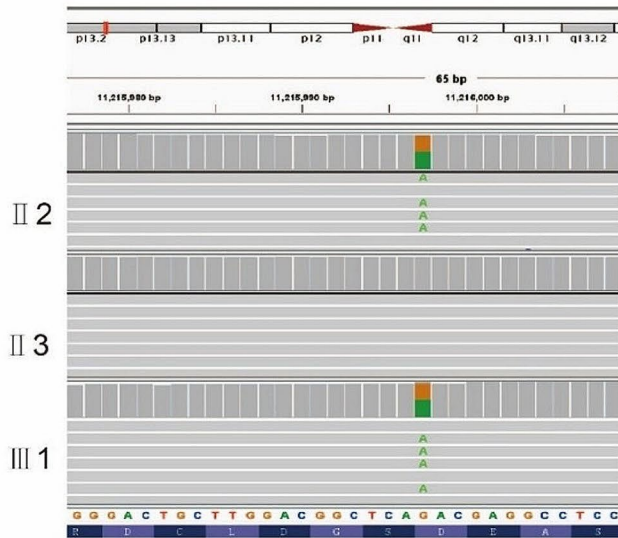
LDLR c.415G > A decreases Dil-LDL absorption by cells

To examine if LDLR c.415G > A impacts protein activity, plasmid-transfected cells were co-incubated with Dil-LDL at 37 °C for at least 4 h. The variant group's red fluorescence was much less than that of the WT group, as shown in Fig. 4, suggesting that the variant group's LDL uptake was noticeably lower than that of the WT group. The capacity to absorb LDL in the blank control group was minimal. These results indicate that LDLR c.415G > A impaired the capacity to absorb LDL significantly.

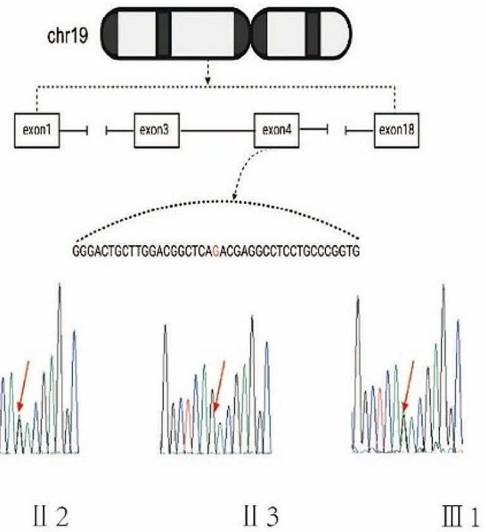
LDLR c.415G > A weakens the ability of LDLR to bind to LDL

The mechanism underlying the lower absorption ability induced by the LDLR c.415G > A variant was further

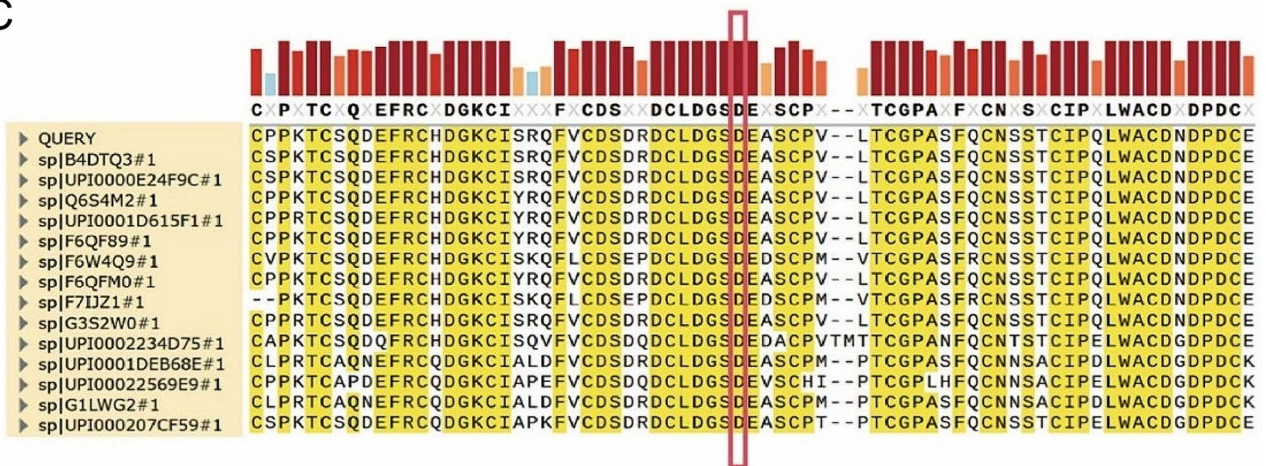
A



B



C



D

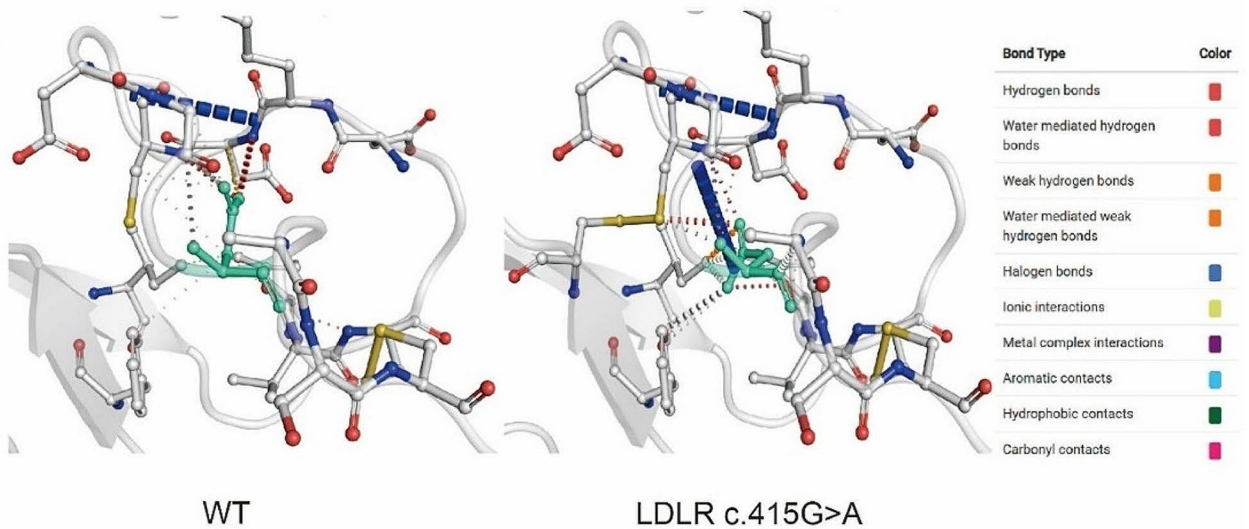


Fig. 2 (See legend on next page.)

(See figure on previous page.)

Fig. 2 Sequencing results and in silico analysis of pathogenic variants. **(A)** Whole-exome sequencing results visualized using Integrative Genomics Viewer (IGV). **(B)** Chromosomal location of *LDLR* c.415G>A and Sanger sequencing results. *LDLR* c.415G>A is shown by the red arrow. The bimodal distribution indicates that the variant is heterozygous. **(C)** Examination of interspecific conservation of homologous proteins. The red box indicates that amino acids are affected by *LDLR* c.415G>A. Amino acids with conservation greater than 90% are highlighted in yellow. **(D)** Differences in interatomic interactions between wild-type and variant LDLR. Wild-type and variant residues are light green and are shown as sticks with adjacent residues involved in the interaction

evaluated using laser confocal microscopy to investigate the ability of LDLR to bind to LDL after co-incubating the plasmid-transfected cells with LDL antibodies and Dil-LDL at 4 °C for 4 h. As shown in Fig. 5, although there was a significant decrease in LDL binding, the LDLR protein content in the variant group was nearly equal to that of the WT group. Therefore, by decreasing LDLR binding to LDL, the variant dramatically lowers the absorption capacity.

Discussion

In this study, serious issues in lipid metabolism were observed in the proband and his son, who carried *LDLR* c.415G>A. This variant was previously described [36] and was included in the ClinVar database. (NM_000527.4(LDLR):c.415G>A (p.Asp139Asn)) as likely pathogenic with accession number RCV000237450.1, but no functional studies have been conducted. The present functional studies revealed that while this variant had no effect on protein synthesis, it dramatically lowered LDL absorption via impairing the ability of LDLR to bind LDL. It is hypothesized that this variant affects the uptake ability of LDLR, inhibiting the regular excretion of LDL-C in plasma and resulting in FH.

Mature LDLR proteins consist of 860 amino acids and can be divided into five functional domains [37]. Among these, the interaction between acidic residues of the LDLR ligand-binding domain and basic residues of apoB100 mediates the binding of LDL to LDLR [38]. The variant detected in this study is located in the ligand-binding domain. The replacement of asparagine with aspartic acid results in distinct molecular interactions with the surrounding residues. This may explain the lack of affinity of the variant protein for LDL. Previous functional studies of pathogenic of *LDLR* variants have revealed that *LDLR* p.L799R disrupts the transmembrane domain, inhibiting membrane insertion and resulting in the secretion of LDLR [39]. *LDLR* p. D482H and C667F were trapped in the endoplasmic reticulum owing to misfolding [40]. *LDLR* p.W23X, S78X, or W541X nonsense mutations significantly decreased the levels of mRNA expression [41]. To sum up, *LDLR* variants can lead to FH by altering different stages of receptor-mediated endocytosis. Certain circumstances may result in the total absence of receptors, whereas other circumstances may result in receptors that are present but with

impaired function. All these will lead to the inability of cells to absorb LDL, which will build up cholesterol in the blood and raise the risk of atherosclerosis. In this family, both the proband and his son exhibited serious problems related to lipid metabolism, although genetic testing showed that they were heterozygous and cell tests demonstrated that the variant did not affect protein expression. Lipid metabolism is closely related to a decline in receptor function.

Even though FH is the most common disease associated with disorders in cholesterol metabolism, it has received fairly little public attention, and its rate of diagnosis is quite poor [6]. Most patients with FH do not receive an effective lipid-lowering medication [42]. Since early myocardial infarction, stroke, and an elevated risk of overall mortality are frequent features of untreated FH, it is well acknowledged that the illness poses a serious risk to life [43]. Therefore, more research is required to improve outcomes for patients with FH and their families.

Study strengths and limitations

The pathogenicity of missense variant *LDLR* c.415G>A was confirmed by this study, which impaired binding and uptake of LDLR to LDL. These findings underpin the early diagnosis of FH, contribute to cascade screening of FH families, and advocate for personalized treatment strategies. However, this study still had some limitations. Firstly, no in vivo functional experiments were conducted. Further evidence from gene-edited murine models to confirm the pathogenicity of the *LDLR* c.415G>A variant is required. Secondly, the assessment of LDLR activity relied solely on one cell line model system, necessitating validation across diverse cell line models to ensure research robustness. Finally, the scope of the current study did not extend to investigating how to address the pathogenicity of this variant. Future studies are required to ameliorate the harmful consequences of variants, which will help achieve more effective lipid-lowering treatments.

Conclusion

LDLR c.415G>A is a pathogenic variant in FH. It causes acidic amino acids to be replaced, greatly reducing the capacity of LDLR to bind to LDL. This prevents LDL-C from being taken up by cells and produces a noticeable LDL-C increase in plasma. This study advances our

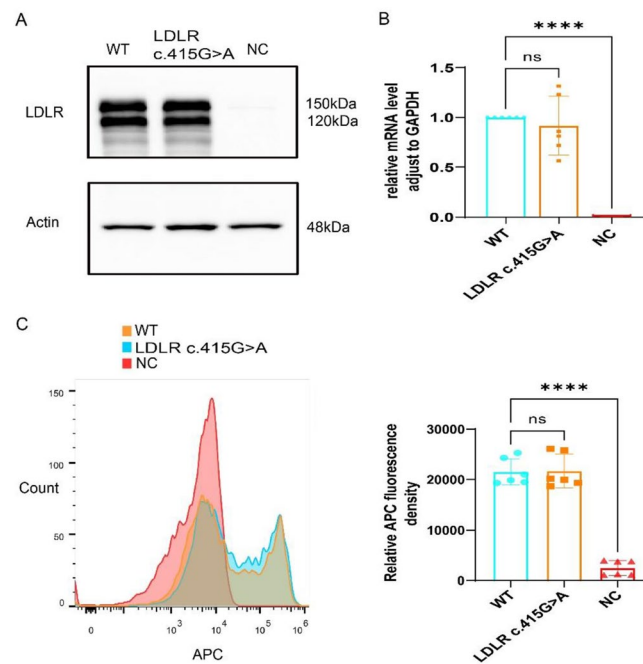


Fig. 3 *LDLR* c.415G>A does not affect LDLR expression. **(A)** Western blot analysis of LDLR expression in HEK293T cells transfected with wild-type LDLR plasmids, variant LDLR plasmids, and blank plasmids. **(B)** Quantitative reverse transcription polymerase chain reaction analysis ($n=6$ /group). **(C)** Flow cytometry quantification of LDLR expression on the HEK293T cell surface ($n=6$ /group). Data are presented as means \pm SEM. **** $P < 0.0001$; ns indicates $P > 0.05$

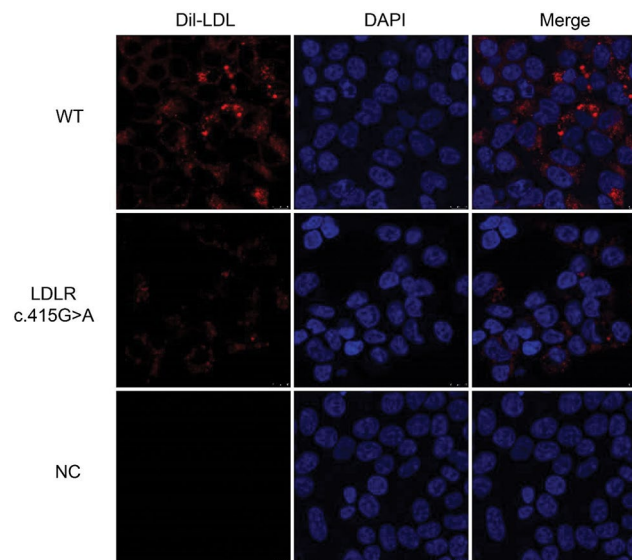


Fig. 4 Capacity of LDLR to absorb LDL, as determined using laser confocal microscopy. Double immunofluorescence staining of LDL (red) and DAPI (blue). Image magnification: 100 \times , scale bar: 10 μ m. WT: wild-type LDLR; NC: negative control

understanding of FH-associated gene variants and identifies a pathogenic variant, providing information that contributes to the study of early diagnosis and treatment of FH.

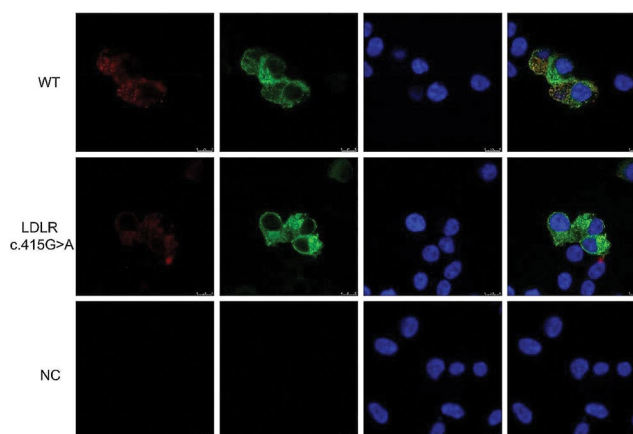


Fig. 5 Ability of LDLR to bind LDL, as determined using laser confocal microscopy. Triple immunofluorescence staining of LDL (red), LDLR (green), and DAPI (blue). Image magnification: 100×, scale bar: 10 μm

Abbreviations

FH	familial hypercholesterolemia
LDL	low-density lipoprotein
LDL-C	low-density lipoprotein cholesterol
LDLR	low-density lipoprotein receptor
PCSK9	proprotein convertase subtilisin/kexin type 9
DLCN	Dutch Lipid Clinic Network
BGI	Beijing Genomics Institution
GATK	Genome Analysis Toolkit
SNP	single nucleotide polymorphism
MUSCLE	multiple sequence comparison by log-expectation
PCR	polymerase chain reaction
qPCR	quantitative real-time PCR
DAPI	4',6-diamidino-2-phenylindole
DiI-LDL	labelled human plasma LDL
WT	wild-type

Supplementary Information

The online version contains supplementary material available at <https://doi.org/10.1186/s12944-024-02068-2>.

Supplementary Material 1: The success rate of transfection. Double immunofluorescence staining of LDLR (green) and DAPI (blue)
Supplementary Material 2: The whole-exome sequencing data of FH related gene
Supplementary Material 3: The certificate of language editing
Supplementary Material 4: The proof report of the overall similarity index
Supplementary Material 5: The image of LDLR and Actin obtained through chemiluminescence
Supplementary Material 6: The image of Marker obtained through colorimetric
Supplementary Material 7: the overlay image of LDLR, Actin and Marker
Supplementary Material 8: Western blot analysis of LDLR expression

Author contributions

X.C and S.L contributed to the supervision, conception, project administration, funding acquisition and final approval of the submitted version. K.W, T.H, and M.T contributed to the methodology, software, analysis, and original draft preparation. H.C and Y.S contributed resources. All authors have read and approved the final manuscript.

Funding

The research was supported by the grants from the Key Technology R&D Program of Ningbo (2022Z149) and the Key Laboratory of Precision Medicine for Atherosclerotic Disease of Zhejiang Province (2022E10026).

Data availability

The datasets presented in this article are not readily available because sharing of genomic data in the public domain is not allowed according to the requirements of the Institutional Ethics Committee. Requests to access the datasets should be directed to the corresponding authors.

Declarations

Ethics approval and consent to participate

This study was approved by the Ethics Committee of the First Affiliated Hospital of Ningbo University (2019-R020), and all participants signed written informed permission forms for participation.

Consent for publication

All participants provided consent for publication.

Competing interests

The authors declare no competing interests.

Received: 5 January 2024 / Accepted: 28 February 2024

Published online: 21 March 2024

References

- Brandts J, Ray KK. Familial hypercholesterolemia: JACC Focus Seminar 4/4. *J Am Coll Cardiol*. 2021;78(18):1831–43.
- Defesche JC, et al. Familial hypercholesterolaemia. *Nat Rev Dis Primers*. 2017;3:17093.
- Ference BA, et al. Low-density lipoproteins cause atherosclerotic cardiovascular disease. 1. Evidence from genetic, epidemiologic, and clinical studies. A consensus statement from the European Atherosclerosis Society Consensus Panel. *Eur Heart J*. 2017;38(32):2459–72.
- Tromp TR, et al. Worldwide experience of homozygous familial hypercholesterolaemia: retrospective cohort study. *Lancet*. 2022;399(10326):719–28.
- Beheshti SO, et al. Worldwide Prevalence of Familial Hypercholesterolemia: Meta-analyses of 11 million subjects. *J Am Coll Cardiol*. 2020;75(20):2553–66.
- Benito-Vicente A et al. *Familial hypercholesterolemia: the most frequent cholesterol metabolism disorder caused Disease*. *Int J Mol Sci*. 2018. 19(11).
- Nordestgaard BG, Benn M. Genetic testing for familial hypercholesterolaemia is essential in individuals with high LDL cholesterol: who does it in the world? *Eur Heart J*. 2017;38(20):1580–3.
- de Ferranti S, Sheldrick RC, Wong JB et al. *Response by de Ferranti to Letter Regarding Article, Prevalence of Familial Hypercholesterolemia in the 1999*

- to 2012 United States National Health and Nutrition Examination Surveys (NHANES). *Circulation*, 2016. 134(18)
9. Watts GF et al. *International Atherosclerosis Society Roadmap for Familial Hypercholesterolaemia*. *Global Heart*, 2024. 19(1).
 10. Hesse R, et al. Familial hypercholesterolemia identification by machine learning using lipid Profile Data performs as Well as Clinical Diagnostic Criteria. *Volume 15. Circulation: Genomic and Precision Medicine*; 2022. 5.
 11. Dharmayat KI, et al. Familial hypercholesterolaemia in children and adolescents from 48 countries: a cross-sectional study. *Lancet*. 2024;403(10421):55–66.
 12. Ahmad ZS, et al. US physician practices for diagnosing familial hypercholesterolemia: data from the CASCADE-FH registry. *J Clin Lipidol*. 2016;10(5):1223–9.
 13. Harada-Shiba M, et al. Guidelines for the diagnosis and treatment of Pediatric Familial Hypercholesterolemia 2022. *J Atheroscler Thromb*. 2023;30(5):531–57.
 14. Goldstein JL, Brown MS. The LDL receptor. *Arterioscler Thromb Vasc Biol*. 2009;29(4):431–8.
 15. Bartuzi P, et al. CCC- and WASH-mediated endosomal sorting of LDLR is required for normal clearance of circulating LDL. *Nat Commun*. 2016;7:10916.
 16. Fedoseienko A, et al. The COMMD Family regulates plasma LDL levels and attenuates atherosclerosis through stabilizing the CCC complex in endosomal LDLR trafficking. *Circ Res*. 2018;122(12):1648–60.
 17. Mousavi SA, Berge KE, Leren TP. The unique role of proprotein convertase subtilisin/kexin 9 in cholesterol homeostasis. *J Intern Med*. 2009;266(6):507–19.
 18. Cesaro A et al. *Beyond cholesterol metabolism: The pleiotropic effects of proprotein convertase subtilisin/kexin type 9 (PCSK9)*. *Genetics, mutations, expression, and perspective for long-term inhibition* *BioFactors*, 2020. 46(3): p. 367–380.
 19. Bottomley MJ, et al. Structural and biochemical characterization of the wild type PCSK9-EGF(AB) Complex and Natural familial hypercholesterolemia mutants. *J Biol Chem*. 2009;284(2):1313–23.
 20. Fan D, et al. Self-association of human PCSK9 correlates with its LDLR-Degrading activity. *Biochemistry*. 2008;47(6):1631–9.
 21. Grefhorst A, et al. Plasma PCSK9 preferentially reduces liver LDL receptors in mice. *J Lipid Res*. 2008;49(6):1303–11.
 22. Viigimaa M, et al. New Horizons in the Pathogenesis, pathophysiology and treatment of familial hypercholesterolaemia. *Curr Pharm Design*. 2019;24(31):3599–604.
 23. Liyanage KE, et al. Familial hypercholesterolemia: epidemiology, neolithic origins and modern geographic distribution. *Crit Rev Clin Lab Sci*. 2011;48(1):1–18.
 24. Abifadel M, Boileau C. Genetic and molecular architecture of familial hypercholesterolemia. *J Intern Med*. 2023;293(2):144–65.
 25. Chiou K-R, Charng M-J. Common mutations of familial hypercholesterolemia patients in Taiwan: characteristics and implications of migrations from south-east China. *Gene*. 2012;498(1):100–6.
 26. Chiou K-R, Charng M-J. Genetic diagnosis of familial hypercholesterolemia in Han Chinese. *J Clin Lipidol*. 2016;10(3):490–6.
 27. Yip M-K et al. *Genetic Spectrum and Cascade Screening of Familial Hypercholesterolemia in Routine Clinical setting in Hong Kong*. *Genes*, 2023. 14(11).
 28. Bourbon M, Alves AC, Sijbrands EJ. Low-density lipoprotein receptor mutational analysis in diagnosis of familial hypercholesterolemia. *Curr Opin Lipidol*. 2017;28(2):120–9.
 29. Benito-Vicente A et al. *Validation of LDLr activity as a Tool to improve genetic diagnosis of familial hypercholesterolemia: a retrospective on functional characterization of LDLr variants*. *Int J Mol Sci*, 2018. 19(6).
 30. Li H, Durbin R. Fast and accurate long-read alignment with Burrows-Wheeler transform. *Bioinformatics*. 2010;26(5):589–95.
 31. McKenna A, et al. The genome analysis Toolkit: a MapReduce framework for analyzing next-generation DNA sequencing data. *Genome Res*. 2010;20(9):1297–303.
 32. Schwarz JM, et al. MutationTaster evaluates disease-causing potential of sequence alterations. *Nat Methods*. 2010;7(8):575–6.
 33. Rodrigues CHM, Pires DEV, Ascher DB. DynaMut: predicting the impact of mutations on protein conformation, flexibility and stability. *Nucleic Acids Res*. 2018;46(W1):W350–5.
 34. Ajith A, Subbiah U. *In silico screening of non-synonymous SNPs in human TUFT1 gene*. *J Genetic Eng Biotechnol*, 2023. 21(1).
 35. Hu J, et al. Human embryonic kidney 293 cells: a vehicle for Biopharmaceutical Manufacturing, Structural Biology, and Electrophysiology. *Cells Tissues Organs*. 2018;205(1):1–8.
 36. Deiana L, Garuti R, Pes GM, Carru C, Errigo A, Rollieri M, Pisciotta L, Masturzo P, Cantafora A, Calandra S, Bertolini S. Influence of beta(0)-thalassemia on the phenotypic expression of heterozygous familial hypercholesterolemia: a study of patients with familial hypercholesterolemia from Sardinia. *Arterioscler Thromb Vasc Biol*. 2000;20(1):236–43.
 37. Jeon H, Blacklow SC. Structure and physiologic function of the low-density lipoprotein receptor. *Annu Rev Biochem*. 2005;74(1):535–62.
 38. Yamamoto T, Davis CG, Brown MS, Schneider WJ, Casey ML, Goldstein JL, Russell DW. The human LDL receptor: a cysteine-rich protein with multiple alu sequences in its mRNA. *Cell*. 1984;31(1):27–38.
 39. Strøm TB, Laerdahl JK, Leren TP. Mutation p.L799R in the LDLR, which affects the transmembrane domain of the LDLR, prevents membrane insertion and causes secretion of the mutant LDLR. *Hum Mol Genet*. 2015;24(20):5836–44.
 40. Kizhakkedath P, et al. Endoplasmic reticulum quality control of LDLR variants associated with familial hypercholesterolemia. *FEBS Open Bio*. 2019;9(11):1994–2005.
 41. Holla ØL, Kulseth MA, Berge KE, Leren TP, Ranheim T. Nonsense-mediated decay of human LDL receptor mRNA. *Scand J Clin Lab Investig*. 2009;69(3):409–17.
 42. Nordestgaard BG, et al. Familial hypercholesterolaemia is underdiagnosed and undertreated in the general population: guidance for clinicians to prevent coronary heart disease: consensus statement of the European Atherosclerosis Society. *Eur Heart J*. 2013;34(45):3478–90a.
 43. Gidding SS, et al. The Agenda for Familial Hypercholesterolemia: A Scientific Statement from the American Heart Association. *Circulation*. 2015;132(22):2167–92.

Publisher's Note

Springer Nature remains neutral with regard to jurisdictional claims in published maps and institutional affiliations.